Published in Journal of Contaminant Hydrology 146, 37-50, 2013
which should be used for any reference to this work

Identification of chlorinated solvents degradation zones in clay till by high resolution chemical, microbial and compound specific isotope analysis

Ida Damgaard [a,*], Poul L. Bjerg [a], Jacob Bælum [b,e], Charlotte Scheutz [a], Daniel Hunkeler [c], Carsten S. Jacobsen [b,f], Nina Tuxen [d], Mette M. Broholm [a]

[a] DTU Environment (Department of Environmental Engineering, Technical University of Denmark), Miljoevej bldn 113, DK-2800 Lyngby, Denmark
[b] Geological Survey of Denmark and Greenland, Ø. Voldgade 10, 1350 København K, Denmark
[c] University of Neuchatel, Rue Emile-Argand 11 – CP 158, CH - 2009 Neuchâtel, Switzerland
[d] Orbicon, Ringstedvej 20, 4000 Roskilde, Denmark
[e] The Technical University of Denmark - Center for Biosustainability, Kogle Allé 6, 2970 Hørsholm, Denmark
[f] University of Copenhagen, Thorvaldsensvej 40, 1958 Frederiksberg C, Denmark

A B S T R A C T

The degradation of chlorinated ethenes and ethanes in clay till was investigated at a contaminated site (Vadsby, Denmark) by high resolution sampling of intact cores combined with groundwater sampling. Over decades of contamination, bioactive zones with degradation of trichloroethene (TCE) and 1,1,1-trichloroethane (1,1,1-TCA) to 1,2-*cis*-dichloroethene (*cis*-DCE) and 1,1-dichloroethane, respectively, had developed in most of the clay till matrix. *Dehalobacter* dominated over *Dehalococcoides* (*Dhc*) in the clay till matrix corresponding with stagnation of sequential dechlorination at *cis*-DCE. Sporadically distributed bioactive zones with partial degradation to ethene were identified in the clay till matrix (thickness from 0.10 to 0.22 m). In one sub-section profile the presence of *Dhc* with the *vcrA* gene supported the occurrence of degradation of *cis*-DCE and VC, and in another enriched $\delta^{13}C$ for TCE, *cis*-DCE and VC documented degradation. Highly enriched $\delta^{13}C$ for 1,1,1-TCA (25‰) and *cis*-DCE (−4‰) suggested the occurrence of abiotic degradation in a third sub-section profile. Due to fine scale heterogeneity the identification of active degradation zones in the clay till matrix depended on high resolution subsampling of the clay till cores. The study demonstrates that an integrated approach combining chemical analysis, molecular microbial tools and compound specific isotope analysis (CSIA) was required in order to document biotic and abiotic degradations in the clay till system.

Keywords:
Chlorinated ethenes
Chlorinated ethanes
Reductive dechlorination
Low permeability
Clay till
Dehalococcoides
Dehalobacter
vcrA
bvcA
CSIA

1. Introduction

The widespread and uncontrolled industrial use of chlorinated solvents such as per- and trichloroethylene (PCE and TCE) and 1,1,1-trichloroethane (1,1,1-TCA) has caused these relatively mobile compounds to be among the most frequently found contaminants in groundwater. When spilled on a fractured media, chlorinated solvents are transported downwards as dense nonaqueous phase liquid (DNAPL) through preferential pathways (e.g. vertical fractures) with following diffusion into the sediment matrix (Falta, 2005; Reynolds and Kueper, 2002). When the concentration level in the fractures is lower than in the matrix slow counter diffusion will start (Parker et al., 2004). Thus, the contaminants are likely to stay in the matrix for several decades (Chambon et al., 2010) and can serve as a long-term secondary source to groundwater contamination of an underlying aquifer (Dearden et al., 2012).

Chlorinated ethenes (PCE and TCE) can undergo reductive dechlorination to ethene (MaymoGatell et al., 1997). The sequential dechlorination requires anaerobic conditions (iron–reducing to methanogenic) (Hoelen and Reinhard, 2004; MaymoGatell et al., 1995; Wei and Finneran, 2011), a hydrogen donor (e.g. lactate, Aulenta et al., 2007) and a certain composition of the bacterial community (Duhamel et al.,

* Corresponding author at: Department of Environmental Engineering, Technical University of Denmark, Miljoevej bldn. 113, DK-2800 Lyngby, Denmark. Tel.: +45 61 18 57 76.
E-mail address: idda@env.dtu.dk (I. Damgaard).

2002). The degradation of PCE and TCE to *cis*-dichloroethene (*cis*-DCE) can be carried out by a variety of halogenating bacteria (such as *Desulfitobacterium*, *Dehalobacter restrictus* (*Dhb*) and *Desulfuromonas* (Middeldorp et al., 1999)), however, the degradation to ethene is only known to be carried out by the *Dehalococcoides* spp. (*Dhc*) (MaymoGatell et al., 1997). *Dhc* containing the gene *tceA* have been found to respire TCE and *cis*-DCE (Seshadri et al., 2005) whereas *Dhc* with the genes *vcrA* or *bvcA* respire *cis*-DCE and vinyl chloride (VC) (Muller et al., 2004; Sung et al., 2006). Several recent laboratory studies have also suggested that abiotic degradation pathways for chlorinated ethenes are of importance in the presence of iron minerals (Darlington et al., 2008; Ferrey et al., 2004; He et al., 2008, 2010; Jeong et al., 2011; Lollar et al., 2010). Biotic and abiotic degradations of chlorinated ethenes and ethanes have been documented by compound specific isotope analysis (CSIA) in several studies (for chlorinated ethenes e.g. Courbet et al., 2011; Hunkeler et al., 2005; Lollar et al., 2001 and for chlorinated ethanes e.g. Lollar et al., 2010).

Chlorinated ethenes and ethanes often occur as co-contaminants at the same sites, because they have been used by the same industries in the past. The degradation of chlorinated ethanes such as 1,1,1-TCA involves a range of biotic and abiotic transformations in subsurface systems as reviewed by Scheutz et al. (2011). The presence of 1,1,1-TCA in combination with chlorinated ethenes complicates the degradation of chlorinated ethenes as 1,1,1-TCA has been found to have an inhibitory effect on the reductive dechlorination of *cis*-DCE and VC (Chan et al., 2011; Duhamel et al., 2002; Grostern and Edwards, 2006; Scheutz et al., 2011).

Natural and enhanced degradation of chlorinated ethenes in high permeability deposits (aquifers) is well known (Hunkeler et al., 2011; Major et al., 2002; Scheutz et al., 2008). In low permeability media, such as clay tills, little is known about how degradation by reductive dechlorination distributes between preferential flow paths such as sand lenses and fractures and the clay till matrix. This is crucial when e.g. looking at the contaminant flux from the clay till to the underlying aquifer (Chambon et al., 2010) or with regard to timeframes of a remediation using enhanced reductive dechlorination (ERD) in clay till (Lemming et al., 2010). A recent study by Takeuchi et al. (2011) documented the presence of *Dhc* in an organic-rich clayey aquitard undergoing natural reductive dechlorination of PCE to ethene. Findings by Scheutz et al. (2010) and Manoli et al. (2011) in studies of ERD of chlorinated ethenes in clay tills at two Danish sites (Rugårdsvej and Sortebrovej) suggest, that *Dhc* are able to spread to the matrix adjacent to induced fractures and natural sand stringers resulting in bioactive zones extending up to 5 cm in the clay till matrix. However, the distribution and expansion of these zones in the matrix have not been investigated/documented.

Investigations were carried out at an old contaminated site (Vadsbyvej, Denmark) where natural attenuation processes (transport, sorption, diffusion and degradation) have occurred for four decades. The objective of this field study was: 1) to evaluate the biotic and abiotic degradations of chlorinated ethenes and ethanes in a clay till matrix with embedded sand lenses, sand stringers and fractures; and 2) to identify the distribution and extent of degradation zones in the clay till matrix using state of the art chemical analysis, molecular microbial tools and compound specific isotope analysis (CSIA). The distribution and extent of potential degradation zones were investigated by high-resolution sampling of intact cores. This study offers the first demonstration of natural attenuation (degradation) of chlorinated ethenes and ethanes in clay till that is documented by three parallel lines of evidence: (1) CSIA evidence of degradation of the chlorinated hydrocarbons, (2) molecular tools that document the presence of indigenous organisms (*Dehalococcoides*, *Dehalobacter*) that can completely degrade chlorinated hydrocarbons to innocuous materials, (3) accumulation of degradation products.

2. Field site

The field site is located in the eastern part of Denmark in Vadsby, Hedehusene. The former use as a chemical distribution center from 1973 to 1976 has caused subsurface contamination primarily with chlorinated ethenes and ethanes but also with water soluble organic contaminants and hydrocarbons (Fig. 1a). Degradation of chlorinated ethenes and ethanes is expected as degradation products (mainly *cis*-DCE and 1,1-dichloroethane (1,1-DCA), but also VC and ethene) and specific degraders *Dhc* were found in the groundwater (Capital Region of Denmark, 2007). Potentially, degradation has been taking place for decades yielding a unique opportunity to investigate the natural progression of degradation zones in the clay till.

Two basal clay till units have been identified at the site: the upper clay till from 0.5–1 to 8–9 m below surface (m b.s.) and the lower clay till from 8–9 to 14–15 m b.s. (Christiansen et al., 2010), Fig. 1b. The oxidized clay till (down to 3–5 m b.s. Fig. 1b) is highly fractured due to freeze and thaw processes and contains many worm and root holes (Christiansen et al., 2008). This is reflected in the contaminant distribution by the presence of chlorinated solvents in most of the clay till matrix. Fewer fractures are present below 3–5 m b.s. (Christiansen et al., 2008). In some places the upper clay till is separated from the lower clay till by sand lenses and stringers, which possibly have resulted in horizontally more widespread contamination around this interface. Below the lower clay till (14–15 m b.s.), alternating layers of clay till, sandy/silty till and local sand lenses deposited from melt water with a thickness varying from 3 to 10 m are found. The sandy layers are in hydraulic contact with the underlying Bryozo chalk, which is densely fractured in the upper part. Hydraulic head measurements at the site showed a downward groundwater gradient from the contaminated clay till to the chalk aquifer (Fig. 1b). This is supported by the presence of contaminants in the sandy/silty layer underneath the clay till. However, only traces of contaminants have been detected in the chalk aquifer.

3. Materials and methods

3.1. Investigative approach

The degradation of chlorinated ethenes and ethanes in the clay till matrix and high permeability features (such as sand lenses, sand stringers and fractures) was evaluated from analysis of chlorinated solvents including CSIA, redox sensitive parameters, donor availability measured as volatile fatty acids (VFA) and presence of bacteria. An overview of all parameters analyzed in groundwater and in the clay till matrix is presented in Appendix A Table S1.

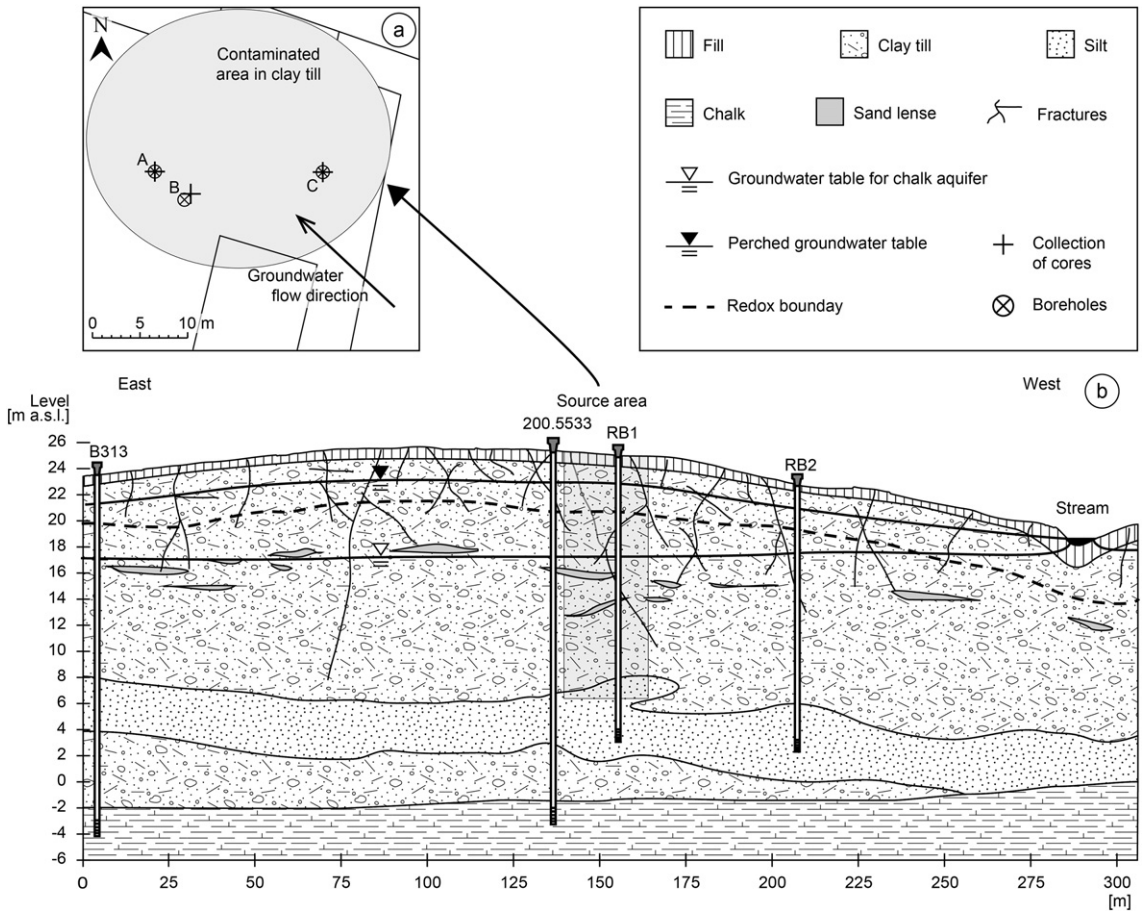

Fig. 1. (a) The source zone at the Vadsby site after investigations carried out in 2007. Boreholes A, B and C and core collection locations from A, B and C are also shown. (b) Vertical cross section illustrating the geological setting north of the site. The source area in the clay till is marked.

The degradation in the clay till matrix was investigated by collecting intact cores from three boreholes in the source area (A, B and C, marked in Fig. 1a). These locations were selected because previous investigations showed different concentration levels and composition of contaminants in these areas. The specific coring depths were selected based on membrane interface probe profiles combined with field GC measurements for each 0.6 m to determine the composition of PCE, TCE and chlorinated degradation products (see further description in Appendix A).

The vertical geochemical and contaminant profiles within the intact cores were sampled with increasing distance to identified geological features by discrete sub-sampling. Concentrations of chlorinated ethenes and ethanes were analyzed for each sampled depth, while the concentrations of redox sensitive parameters and VFA were analyzed for selected depths. Potentially bioactive zones were identified and selected for analysis of microbial degraders and CSIA. The geochemistry and contaminant concentrations in high permeability features (such as sand stringers, sand lenses and fractures) were investigated by sampling of screens installed in the boreholes in the clay till. Due to the higher hydraulic conductivity in the high permeability features compared to the clay till matrix water representing these features could be collected.

3.2. Collection of intact cores

In total 19 intact cores from the three boreholes A, B and C were collected (in total 9.5 m, specific depths can be seen in Appendix A, Table S2) in stainless steel tubes with a diameter of 0.07 m and a length of 0.5 m. The core collection depths were reached by 6 in. dry rotation drilling. After withdrawal the cores were quickly sealed with rubber stoppers, wrapped in Rilsan bags (polamide 11) and closed with tape to minimize volatilization of contaminants and to maintain redox conditions. The cores were stored at 10 °C until sub-sampling in the laboratory.

3.3. Screen installation and collection of groundwater samples

To sample groundwater from permeable features in the clay till GeoProbe Pro Forma 13103 pre-packed screens (0.5 in.–13 mm ID) were installed in borehole A (5.1–6.0 and 8.1–9.0 m b.s.) and C (5.5–5.8, 8.0–8.9 and 11.1–12.0) after the cores were collected. Groundwater from the clay till representing borehole B was collected from an existing well B (screened from 11.0–13.0 m b.s.) (see location in Fig. 1a). In the wells A and C groundwater samples were pressurized to the surface by nitrogen. In well B groundwater was collected using a MP1 pump and dedicated tubing.

Two well and gravel pack volumes were purged prior to collection of samples. Field parameters (pH, dissolved oxygen and EC) were measured by installing WTW instruments in a in-line flow-through cell (pH 330/SET, OX 330/SET and LF 330/SET). Water samples for analysis of concentration and carbon isotope fractionation of chlorinated solvents, redox sensitive parameters and VFA (specific compounds and number of samples are presented in Appendix A, Table S1) were collected from an in-line 3-way valve using a syringe and transferred directly into vials stored at 4 °C until analyzed except VFA samples which were frozen (−18 °C). Microbial samples were collected by decanting 500 mL of groundwater into 0.22 μm polyethersulfone filter units (MoBio, Carlsbad, USA) and vacuum filtrated in the field. The filters were quickly transferred into 2 mL microcentrifuge tubes and snapshot frozen in liquid nitrogen and stored at −80 °C until further processing.

3.4. Discrete sampling of cores

The cores were sub-sampled in the laboratory using the procedure described in detail by Scheutz et al. (2010). The core was extruded from the stainless steel tube into Rilsan and transferred to a fume hood. The length of the core was measured to correlate the actual core length with the sampled depth interval. Smeared materials were carefully removed using a knife. A detailed geological description was made observing sediment type, color, hardness, fractures, sand lenses and sand stringers.

Sub-samples were collected with intervals increasing with distance from the observed fracture, sand lenses or sand stringer (starting with 0.5 cm and increasing to 5 cm intervals). The sub-samples were taken using cork bores; a cork bore with 0.55 cm in diameter for samples for analysis of chlorinated solvents and methane, ethene and ethane (~0.5 g of sample) and a cork bore with a diameter of 1 cm for samples for analysis of carbon isotope fractionation and iron speciation (~3–4 g of sample). Samples for VFA and redox sensitive parameters were cut with a knife from the center of the core (5 g of sample). Microbial samples were collected with a cut-off sterile syringe and quickly transferred into a 2 mL vials containing G2 blocking agent (GEUS, Copenhagen, Denmark). G2 blocking agent was used to coat clay particles to avoid DNA loss during later cell lysis. The samples were immediately stored at −80 °C to preserve mRNA.

From each core an intact core slice of approximately 5 cm was weighed just after it was sampled and dried at 105 °C to constant weight. The porosity (ε) and dry bulk densities (ρ_d) were calculated assuming water saturation and a grain density for silica ($\rho_s = 2.65$ g/cm^3) (results are given in Appendix A, Table S3).

3.5. Chemical extraction and analysis

Analysis of groundwater samples was carried out according to Scheutz et al. (2010). The protocol described by Scheutz et al. (2010) was used for extraction and analysis of sediment samples (for chlorinated ethenes and ethanes, NVOC, VFA and redox sensitive parameters); however, with minor modifications (described in Appendix A). Samples for analysis of solid phase Fe(III) were transferred into 10 mL nitrogen flushed glass vials. The vials were capped and stored at −18 °C until analyzed. The procedure for extraction of Fe(II) and Fe(III) was developed based on Heron et al. (1994) and Lovley and Phillips (1987). Extractions were made on approximately 2 g of clay till suspended in 10 mL of anaerobic oxalate solution. The anaerobic oxalate solution was added to the vials in an anaerobic glovebox (Coy®). Fe(II) concentrations in the extract were analyzed on a Varian Cary 50 Bio UV–visible spectrophotometer (Santa Clara, United States) using ferrozine (2 mL of 5.4 g/L ferrozine to approximately 0.2 mL oxalate extract) and an acetate buffer at pH 5. Dissolved iron was measured on a Perkin Elmer Instruments AAnalyst 2000 Atomic Absorption Spectrometer (ASS) with flame detection at a wave length at 248.33 nm. The detection limit was 7.2 μg/L.

3.6. Microbial extraction and analysis

The frozen filters from groundwater samples were pulverized in the microcentrifuge tube using a sterile stick, 0.5 mL G2 blocking agent (GEUS, Copenhagen, Denmark) was added and samples were refrozen in liquid nitrogen. Making sure the samples remained frozen; they were freeze dried along with sediment samples over night. ~1 g 1.4 mm ceramic beads (MoBio, Carlsbad, USA) were added and DNA/RNA extraction was performed as described by Damgaard et al. (2012) (see Appendix A). DNA was also extracted using commercial Powerlyzer soil kit (Mobio, Carlsbad, USA) following the manufacturers recommendations, except the samples were pretreated with G2 blocking agent (described in Appendix A). For the groundwater samples the commercial Rapid Water kit (Mobio, Carlsbad, USA) was used also following the manufacturers recommendations, except these samples were also pretreated with G2 blocking agent. In ground water samples, the activity of specific degraders for the VC reductase genes was calculated as the ratio between the measured amount of mRNA and DNA in the sample. No mRNA was detected in any of the sediment samples. Quantitative real-time PCR was performed targeting Dhc specific 16S rRNA genes, *Dehalobacter* spp. (*Dhb*) specific 16S rRNA genes, as well as the functional genes vcrA, bvcA. qPCR was performed in 20 μL reactions of 10 μL SsoFast™ EvaGreen® Supermix (BioRad, Hercules, USA), 0.4 mM of the primers (presented in Appendix A Table S5, MWG, Ebersberg, Germany), 1 μg bovine serum albumine (New England Biolabs, Ipswich, MA, USA), 1 μL extracted DNA and PCR grade water to a final volume of 20 μL. The qPCR protocol was as follows: 98 °C for 2 min (enzyme activation) followed by 50 cycles of 98 °C for 10 s (denaturation) and a combined annealing elongation step for 20 s at the temperature given in Appendix A Table S5. Amplicon specificity was confirmed by a melting curve analysis consisting of 96 cycles of a 0.4 °C increase starting at 58 °C.

3.7. CSIA on groundwater and sediment core samples

The isotope fractionation sediment samples were collected in 20 mL GC/MS purge and trap vials containing 15 mL of water conserved with HCl corresponding to a pH of 2. The sample was stored in a rotating box over night to suspend the sediment in the water then the samples were stored at 10 °C until analysis. Carbon isotope ratios of chlorinated ethenes and ethanes in groundwater and the liquid phase from the sediment extraction vial were analyzed by a Thermo Trace gas Chromatograph

coupled to a Thermo Delta plus XP Isotope-Ratio Mass Spectrometer (IRMS) via a combustion III interface (Thermo Fisher). The samples were pre-concentrated with a purge-and-trap concentrator (Tekmar Velocity XPT, USA) equipped with a VOCARB 3000 trap and connected to a cryogenic trap (ATAS GL, Netherlands) installed inside the GC oven. The analytical procedure reported by Damgaard et al. (2012) was used (also described in Appendix A). Carbon isotope ratios are reported in the delta notation relative to VPDB as defined by $\delta = (R/R_{std} - 1) \times 1000$ [‰], where R and R_{std} are the isotope ratio of the sample and the standard, respectively.

The most depleted $\delta^{13}C$ value for TCE (−30.7‰, Table 1) was found in the deeper screen in well A where TCE in groundwater exceeded 1% of its effective solubility (Table 1). This isotope ratio probably reflects the source isotope signature for TCE ($\delta^{13}C_0$). The value is within the range of carbon isotope ratios reported for measurements on different manufacturer batches (Hunkeler et al., 2008). The value is rather low compared to other sites with high TCE concentrations (e.g. ~−27‰ or ~−25‰ reported by Lollar et al. (2001) and Chartrand et al. (2005), respectively). No $\delta^{13}C$ values for 1,1,1-TCA are available from the location. Based on values reported by Hunkeler et al. (2008) the source isotope signature for 1,1,1-TCA can be expected to be in the range of −25 to −32‰.

3.8. Data treatment

Pore water concentrations of chlorinated ethenes and ethanes, VFA and anions in the sediment samples were calculated from phase partitioning calculations. Sorption distribution coefficients (K_d-values) reported by Lu et al. (2011) were used for estimating sorption of chlorinated compounds. VFA and anions were assumed not to sorb to the sediment.

The reductive dechlorination of chlorinated ethenes and ethanes was evaluated from molar concentrations, molar fractions and the degree of dechlorination (DOD). DOD was calculated separately for the chlorinated ethenes and ethanes from the molar concentrations of the mother compound (PCE, TCE and 1,1,1-TCA) and degradation products (1,2-*cis*-DCE, 1,2-trans-DCE, 1,1-DCE, 1,1-DCA, CA, ethene and ethane) (see Appendix A). A high DOD express that the higher chlorinated compounds have been degraded to lower chlorinated

Table 1
Total concentrations of chlorinated ethenes and ethanes, electron donor, redox-sensitive parameters and microbial numbers in groundwater samples from boreholes A, B and C.

	Borehole	A		B	C		
	Screen depth (m b.s.)	5.1–6	8.1–9	11–13	5.5–5.8	8–8.9	11.1–12
Chlorinated solvents	PCE (μmol/L)	BD	BD	BD	BD	BD	0.2
	TCE (μmol/L)	4	251	0.4	1	1	0.1
	cis-DCE (μmol/L)	3210	2580	354	388	14	0.2
	VC (μmol/L)	139	9	167	11	3	BD
	Ethene (μmol/L)	44	18	160	12	6	0.1
	1,1,1-TCA (μmol/L)	BD	BD	0.3	BD	BD	BD
	1,1-DCA (μmol/L)	824	1064	1065	262	61	7
	CA (μmol/L)	0.8	10	0.3	0	1	BD
	DOD—ethenes	0.35	0.30	0.57	0.36	0.52	0.47
	DOD—ethanes	0.33	0.33	0.33	0.33	0.35	0.33
	Cl (mg/L)	58	213	224	80	552	419
	$\delta^{13}C$ TCE (‰)	BD	−30.7	BD	BD	BD	BD
	$\delta^{13}C$ *cis*-DCE (‰)	−26.9	−24.0	−4.8	−16.1	−15.7	BD
	$\delta^{13}C$ 1,1-DCA (‰)	−20.6	−19.1	−20.6	−21.8	−21.3	−24.3
Electron donor	Total VFA[b] (mg C/L)	42	110	74	2	0.2	0.4
	Hydrocarbon (μg/l)	6.7	55	745	–[a]	0.71	0.150
	Methanol (μg/l)	8.6	<0.025	0.011	–[a]	<0.025	<0.025
	Ethanol (μg/l)	1.2	2.8	BD[c]	–[a]	<0.010	<0.010
	Iso-propanol (μg/l)	13	56	BD[c]	–[a]	0.007	<0.001
	n-propanol (μg/l)	11	180	320[c]	–[a]	0.150	0.086
	Acetone (μg/l)	13	23	<0.05[c]	–[a]	0.013	0.0024
Redox parameters	NO_3-N (μmol/L)	BD	BD	BD	BD	BD	BD
	Fe (dissolved) (mmol/L)	537	752	484	179	179	7
	Mn (dissolved) (μmol/L)	36	18	18	7	9	5
	SO^4-S (μmol/L)	841	904	BD	624	998	1683
	S^{2-} (μmol/L)	5.3	4.0	1.6	BD	2,8	4.3
	CH_4 (μmol/L)	62	BD	187	0	0	0
Microbiology	16S (cells/L)	1.4×10^6	1.1×10^7	BD	1.4×10^6	1.1×10^7	4.4×10^6
	Dhc (cells/L)	BD	BD	2.1×10^7	8.4×10^4	1.5×10^7	BD
	Geo (cells/L)	BD	BD	BD	BD	BD	BD
	Dhb (cells/L)	BD	BD	2.5×10^6	1.3×10^6	2.4×10^5	3.4×10^5
	vcrA (DNA/L)	BD	BD	1.6×10^7	BD	1.1×10^8	5.1×10^6
	bvcA (DNA/L)	BD	BD	3.5×10^4	BD	1.5×10^4	BD
	vcrA (mRNA/DNA)	BD	BD	17	BD	10	10
	bvcA (mRNA/DNA)	BD	BD	3	BD	BD	BD

BD—Below detection limit.
[a] Not enough water for sampling.
[b] Sum of acetate, propionate, formate and lactate.
[c] Analyzed by Orbicon (Capital Region of Denmark, 2007).

compounds and a DOD of 1 express complete dechlorination. Whereas when PCE is the mother compound complete degradation to *cis*-DCE gives a DOD of 0.5 whereas complete degradation of TCE to *cis*-DCE gives a DOD of 0.33.

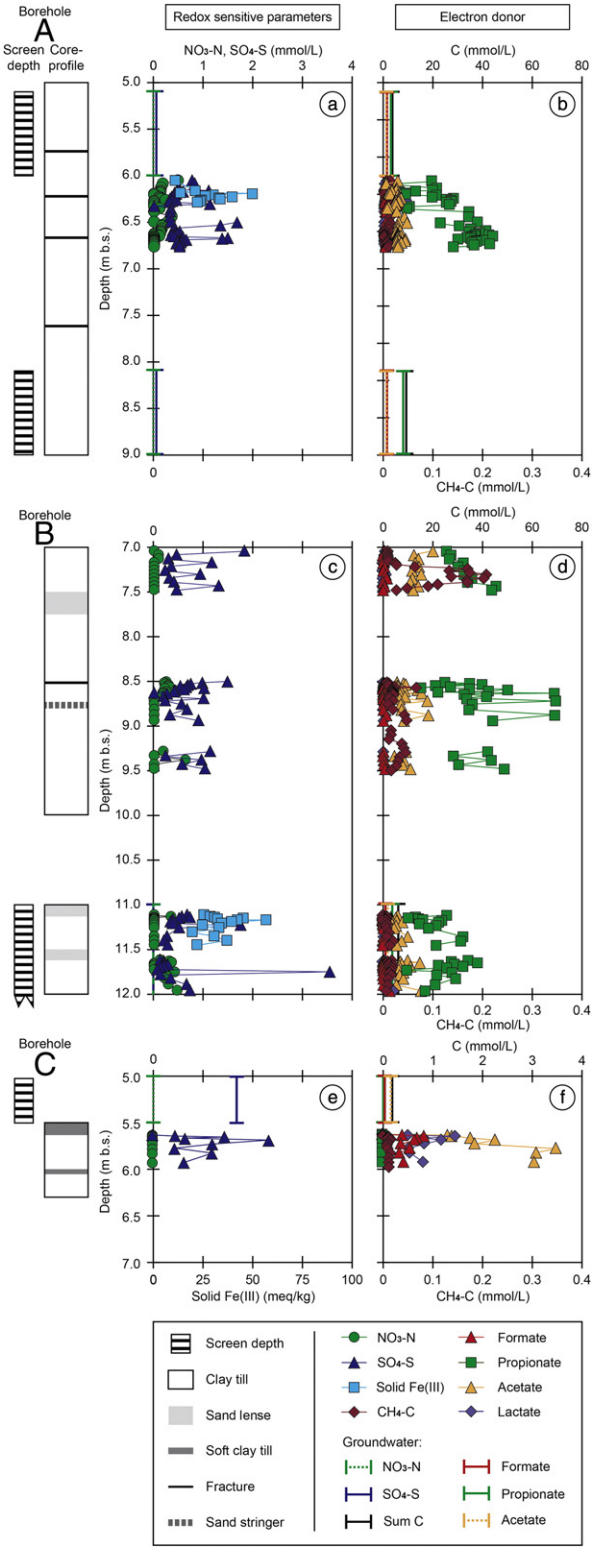

4. Results and discussion

4.1. Geology and biogeochemical conditions in the high permeability features and clay till matrix

The geological log in the 3 boreholes based on drilling and core observations showed similar layering (Fig. 2, locations of boreholes are shown in Fig. 1a). The reddish-brown oxidized zone was fractured and with a large number of bio pores whereas the clay till below the redox boundary was olive gray, massive with few fractures and sand stringers. As the redox boundary in borehole A was situated deeper (4.3 m.b.s) than in B and C (3.3 m b.s.) fractures and biopores were deeper in this borehole. The reduced (gray) clay till was weakly silty and sandy with few gravel and chunks of chalk. Typical clay content of the clay till was around 23–27% dry weight (Lu et al., 2011).

The concentrations of chlorinated ethenes and ethanes, redox parameters and VFA in the clay till matrix (given as pore water concentrations) and in high permeability features (represented by groundwater samples from well screens) in boreholes A, B and C are presented in Figs. 2 and 3. Specific depths of identified geological features (fractures, sand lenses and stringers) in the intact cores are presented in Appendix A, Table S4.

4.1.1. Donor availability

A higher content of VFA was observed in the groundwater and the pore water from boreholes A and B compared to borehole C (Fig. 2, b, d and f). In the pore water from boreholes A and B propionate (up to 70 mmolC/L) and acetate (up to 20 mmolC/L) were found, while mainly acetate was found in well C (3 mmol/L). Similar results were observed in the groundwater. However, the concentrations in the groundwater were much lower (up to 8 mmolC/L in boreholes A and B and up to 0.2 mmol/L in borehole C) indicating faster VFA degradation or dilution in the flowing groundwater in the fractures, sand lenses and sand stringers. These results suggest lower generation of VFA in borehole C compared to A and B. Compared to sites undergoing ERD (Damgaard et al., 2012; Manoli et al., 2011; Scheutz et al., 2010) the concentrations of VFA measured in boreholes A and B are surprisingly high. However, several alcohols (methanol, ethanol, iso-propanol and n-propanol), hydrocarbons and NVOC were found in the groundwater from wells A and B (Table 1). Only few of these compounds were detected in well C (Table 1). Most likely the high concentrations of VFA have been produced during fermentation of the organic contaminants.

4.1.2. Redox conditions

The redox-sensitive parameters measured in the clay till matrix and groundwater indicate that the redox conditions were iron -reducing to methanogenic (Table 1 and Fig. 2a, c and e). The measured concentrations of reduced iron in the

Fig. 2. Concentrations of redox sensitive parameters and VFA measured in groundwater samples from each well screen and calculated pore water concentrations in the clay till matrix in profiles from boreholes A, B and C. Redox sensitive parameters and VFA are measured in selected sub-sections in the cores. The geological composition based on drilling observations and intact core descriptions are also illustrated. Notice secondary axis for methane and different axes for VFA in borehole C. Location of the three boreholes and core collection points can be seen in Fig. 1a.

groundwater from the screens in boreholes A, B and C and in the clay till matrix indicate iron reduction. Sulfate was found in all of the clay till matrix and in the screens from boreholes A and C. The conditions in the screen from borehole B were more reduced as no sulfate was detected and methane production was observed (Table 1).

The redox conditions indicate that reductive dechlorination of chlorinated ethenes and ethanes can proceed (e.g. Heimann et al., 2005; Wei and Finneran, 2011). Several studies suggest that chlorinated ethenes and ethanes can undergo abiotic degradation through reactions with reduced iron minerals (e.g. green rust or FeS) (Ferrey et al., 2004; He et al., 2008; Jeong et al., 2011; Liang et al., 2007). As the sediment is rich in reducible iron oxides (Fig. 2a and c) and sulfate, there is a high potential for biotically reduced reactive iron minerals which can induce abiotic degradation of chlorinated ethenes and ethanes.

4.1.3. Spatial distribution of chlorinated ethenes and ethanes

The observed concentrations of chlorinated ethenes and ethanes and degradation products in the high permeability features and clay till matrix reveal a very diverse and heterogeneous distribution and degradation of contaminants in the three boreholes even after several decades of contamination (Fig. 3). TCE was the dominant chlorinated ethene in a large part of the clay till matrix in the profile from borehole A, where also the highest concentrations of chlorinated ethenes were observed (up to 5000 μmol/L, Fig. 3a). The measured TCE concentrations correspond to more than 1% of the effective solubility of TCE (8400 μmol/L at 20–25 °C, ESTCP, 2004) indicating current or previous presence of residual phase TCE. PCE (only in profile from borehole C) and TCE were only found in small sections of the intact cores from boreholes B and C (Fig. 3c and e). In profiles from boreholes B and C the concentration levels of chlorinated ethenes were lower and *cis*-DCE was dominating. These results reveal that PCE and TCE dechlorination to *cis*-DCE has progressed in most of the profile from boreholes B and C whereas dechlorination of TCE to *cis*-DCE is restricted to the upper part of profile A. The presence of VC and ethene in the groundwater from all three wells and in sporadic sections of the clay till matrix (profile A: 5.0–6.0 m b.s.; profile B: 7.0–7.5, 8.5–9.5 and 11.0–12.0 m b.s.; profile C: 5.5–6.5 m b.s.; Fig. 3a, c and e) indicates that bioactive zones with reductive dechlorination to ethene occur both in the high permeability features and the clay till matrix. However, the *cis*-DCE degradation is the rate limiting step of the dechlorination and is apparently slow as the concentration levels of VC and ethene are low compared to concentration levels of *cis*-DCE. An exception is seen in the screen in borehole B (11–13 m b.s.) where DOD for TCE is 0.52.

In all clay till matrix cores and groundwater samples from boreholes A, B and C, 1,1-DCA was the dominating chlorinated ethane (Fig. 3b, d and e). 1,1,1-TCA was only detected in few sediment samples from borehole B (Fig. 3d), in which the concentration level of 1,1-DCA was higher (up to 1000 μmol/L) than in profiles from boreholes A and C (up to 500 μmol/L) (Fig. 3d and f). The presence and dominance of 1,1-DCA show that 1,1,1-TCA dechlorination to 1,1-DCA has taken place at all borehole locations (A, B and C).

4.2. Detailed evaluation of degradation

Degradation of PCE, TCE and 1,1,1-TCA in selected sub-section profiles of the intact cores was further investigated through use of CSIA and analysis of *Dhb*, *Dhc* and VC reductase genes *vcrA* and *bvcA*. The activity of *Dhc* was investigated through analysis of mRNA in the clay till matrix and groundwater representing high permeability features in the clay till. mRNA was only detected in the groundwater samples and not in any of the sediment samples. Currently, it is not known if the presence and activity of *Dhc* in water samples compared to sediment samples also expresses an analytical bias related to the different sample types (e.g. higher sensitivity in water samples). The groundwater samples integrate microbial presence and activity over depth (well B screen length 2 m and 0.5–0.9 m in wells A and C) whereas sediment samples only represent 5 g of sediment. A limitation with sediment analysis of mRNA is that mRNA is difficult to extract as it strongly sorbs to the sediment (Chamier et al., 1993).

4.2.1. Degradation of TCE to cis-DCE at high concentrations in the clay till matrix

The intact cores from 6.00 to 6.80 m b.s. in borehole A consisted of massive and firm clay with two fractures identified in 6.22 and 6.67 m b.s. (Fig. 4). The very high TCE concentration level in the core samples reflects high sorbed concentrations and potential presence of DNAPL (residual TCE) in high permeability features (Fig. 4A1). If degradation of TCE only takes place in the dissolved phase, i.e. degradation of TCE is desorption and/or dissolution limited, the $\delta^{13}C$ of TCE in both dissolved phase, sorbed phase and DNAPL will remain similar to the expected source signature even when a large fraction has been degraded to *cis*-DCE. It can also result in $\delta^{13}C$ of *cis*-DCE approaching the source signature for TCE, which would otherwise indicate near complete degradation of TCE (or further degradation of *cis*-DCE) (Hunkeler et al., 2008). The high concentration levels of TCE and similar $\delta^{13}C$ of TCE and *cis*-DCE in the core (TCE ~ −30‰, *cis*-DCE ~ −30‰ from 6.30 m b.s. and down, Fig. 4A3) and concurrent presence of the degradation product *cis*-DCE in high concentrations suggest that TCE degradation is dissolution or desorption limited. The presence of *cis*-DCE throughout the sub-section profile indicates that reductive dechlorination of TCE to *cis*-DCE potentially takes place in all of the sub-section profile (Fig. 4A1). However, the concentration profile of *cis*-DCE might also indicate diffusive transport of *cis*-DCE from the section above 6.30 m b.s. to the deeper part. From 6.00 to 6.30 m b.s. the concentrations of the chlorinated ethenes indicate an active sub-section with partial degradation to ethene. This is indicated as TCE is completely degraded to *cis*-DCE from 6.00–6.18 m b.s. and partial degradation to VC is observed in the same sub-section (up to 70 μmol/L). Ethene is only observed below the fracture at 6.22 m b.s. Potentially, ethene could be produced in the entire sub-section above 6.22 m b.s. However, microbial oxidation during sulfate or iron reduction (Kniemeyer et al., 2007) or diffusive loss to fractures may have resulted in ethene depletion. Degradation of TCE and *cis*-DCE in the sub-section is documented by the enriched $\delta^{13}C$ values for TCE and *cis*-DCE (Fig. 3A3). The $\delta^{13}C$ values of *cis*-DCE and the absence of VC and ethene below 6.30 m b.s. indicate no further degradation of *cis*-DCE.

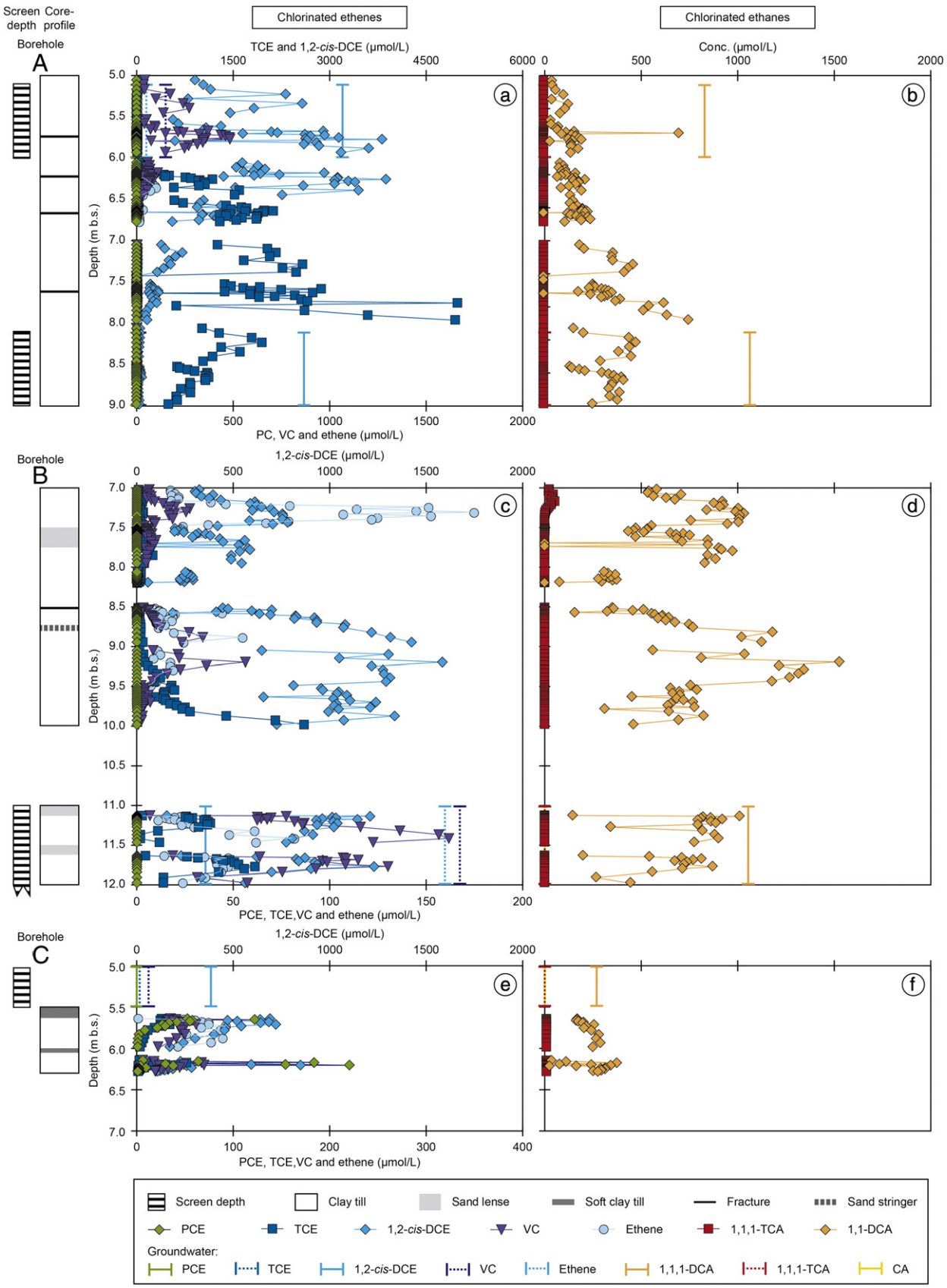
Screen depth
Core-depth profile
Borehole
A
Chlorinated ethenes
Chlorinated ethanes
TCE and 1,2-cis-DCE (µmol/L)
Conc. (µmol/L)
Depth (m.b.s.)
PC, VC and ethene (µmol/L)
a
b
Borehole
B
1,2-cis-DCE (µmol/L)
c
d
PCE, TCE,VC and ethene (µmol/L)
Borehole
C
e
f
Screen depth
Clay till
Sand lense
Soft clay till
Fracture
Sand stringer
PCE
TCE
1,2-cis-DCE
VC
Ethene
1,1,1-TCA
1,1-DCA
Groundwater:
PCE
TCE
1,2-cis-DCE
VC
Ethene
1,1,1-DCA
1,1,1-TCA
CA

In the active sub-section from 6.00 to 6.30 m b.s. reductive dechlorination of TCE to *cis*-DCE and *cis*-DCE to VC and ethene is supported by the presence of *Dhb* and *Dhc* and VC reductase gene *vcrA* respectively (Fig. 3A2) in one sample. Surprisingly, *Dhb* and *Dhc* were not detected in other samples from the sub-section though the concentrations of degradation products and isotope fractionation strongly indicated degradation. The absence in this part cannot be explained. Corresponding to the concentration profiles and isotope fractionations, *Dhb* and *Dhc* were not detected from 6.30 m b.s. and down. In this part the absence of *Dhb* and *Dhc* could be due to high concentrations levels of chlorinated ethenes that can have an inhibiting or toxic effect to the bacteria (Amos et al., 2007; Duhamel et al., 2002; Sabalowsky and Semprini, 2010).

No *Geo*, *Dhb*, *Dhc* or *vcrA* genes were detected in the groundwater from any of the screens in A (5.10–6.00 and 8.10–9.00 m b.s.) (Table 1). The total number of 16S genes shows that other microbes were present (Table 1). As a broad range of microbes are able to reductively dechlorinate TCE to cis-DCE (review by Middeldorp et al., 1999), biotic degradation of TCE potentially takes place in high permeability features. However, degradation to VC and ethene does not seem to occur, though donor is present (Table 1), suggesting that VC and ethene present in the high permeability features are transported there likely by diffusion from the clay till matrix where VC and ethene seem to be produced in minor areas (e.g. 6.00–6.30 m b.s.). This corresponds to decreasing concentrations of VC and ethene around the fracture in 6.22 (Fig. 4A1).

To summarize, reductive dechlorination of TCE primarily to *cis*-DCE but also further to VC and ethene is observed in a 0.30 m sub-section. The degradation is confirmed by enriched $\delta^{13}C$ values for TCE and *cis*-DCE and the presence of *Dhb* and *Dhc* with VC reductase *vcrA* in one sample. High concentrations and the similar $\delta^{13}C$ values for TCE and *cis*-DCE indicate desorption of TCE from the sediment below the section with reductive dechlorination.

4.2.2. Biotic and abiotic degradations of TCE and 1,1,1-TCA in the clay till matrix

The clay till from 7.00 to 7.50 m b.s. in borehole B was firm and massive without any fractures and sand stringers (Fig. 5). *cis*-DCE was the dominating compound in the sub-section profile indicating that TCE has been degraded by reductive dechlorination (Fig. 5B1). Potentially, the reductive dechlorination of TCE to *cis*-DCE has been carried out by *Dhb* as these are present in the sub-section profile (Fig. 5B3) (Middeldorp et al., 1999). Down to 7.20 m b.s. the concentration level of 1,1,1-TCA (40 µmol/L) (Fig. 5B2) is higher than the biotic inhibition level reported by Duhamel et al. (2002) and Chan et al. (2011) (5.2 µmol/L and 0.2–2 µmol/L, respectively). The concurrent lack of VC and ethene suggests 1,1,1-TCA inhibition of *cis*-DCE degradation. The concentration profile of VC and ethene from 7.20 to 7.45 m b.s. indicates an active sub-section with degradation to ethene (Fig. 5B1). This corresponds to the depth where the conditions appear to be more reduced

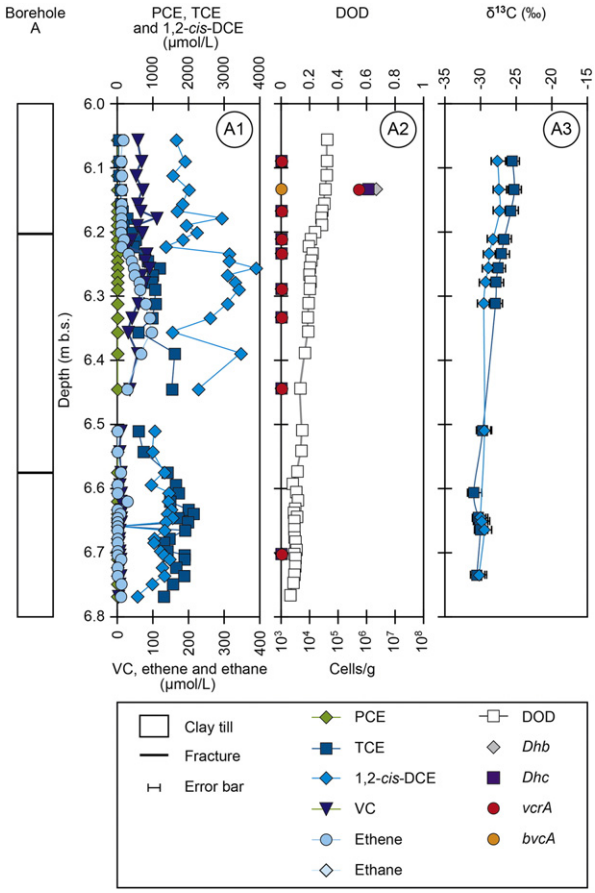

Fig. 4. Sub-section profile from borehole A, 6–6.8 m b.s. Pore water concentration of chlorinated ethenes (A1), calculated DOD for ethenes (from TCE) and presence of Dhb, Dhc, vcrA and bvcA (A2), and $\delta^{13}C$ for TCE and *cis*-DCE (A3). Please note that VC and ethene are on a secondary axis.

(presence of methane, Fig. 2d). The $\delta^{13}C$ value for VC found in one sample (−27‰) could suggest that VC is produced from enriched *cis*-DCE (Fig. 4, B4). The higher concentration of ethene compared to VC indicates that VC possibly is rapidly degraded to ethene or more likely that ethene is not produced from biotic reductive dechlorination but rather from degradation of acetylene to ethene from abiotic degradation of *cis*-DCE (Lee and Batchelor, 2002a, 2002b). However, the dominance of *cis*-DCE and the low concentration of VC and ethene show that only partial degradation has taken place (Fig. 5B1) which may explain that *Dhc* was below the detection limit (Fig. 5B3).

The strong enrichment of $\delta^{13}C$ in *cis*-DCE documents that *cis*-DCE is degraded (Fig. 5B4). In fact the $\delta^{13}C$ for *cis*-DCE is higher than expected for biodegradation considering that *cis*-DCE is the dominating compound and that only low concentrations of VC and ethene are measured (Hunkeler et al. (2008) have reported enrichment factors between −14‰ and −21‰). This suggests that abiotic degradation processes may have contributed to the degradation of TCE and/or *cis*-DCE

Fig. 3. Concentrations of chlorinated ethenes and ethanes measured in groundwater samples from each well screen and calculated pore water concentrations in the clay till matrix in boreholes A, B and C. The geological composition based on drilling observations and intact core descriptions are also illustrated. Notice secondary axis for concentrations of chlorinated ethenes. Location of the three boreholes and core collection points can be seen in Fig. 1a.

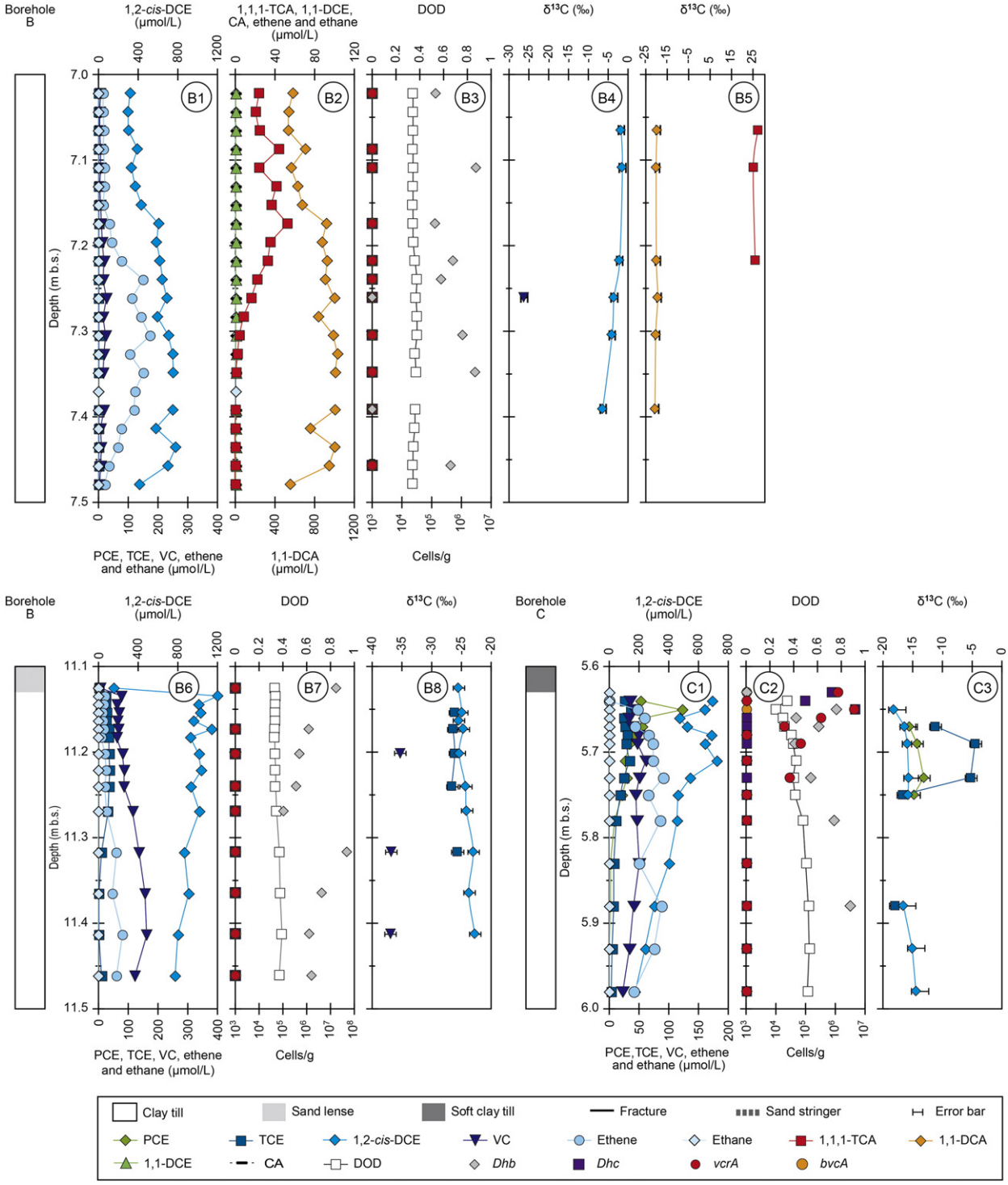

Fig. 5. Sub-section profiles from borehole B (7–7.5 and 11.1–11.5 m b.s.) and borehole C (5.6–6 m b.s.). Pore water concentration of chlorinated ethenes (B1, B6 and C1) and ethanes (B2), calculated DOD for ethenes (calculated from TCE in B and PCE in C), presence of Dhb, Dhc, vcrA and bvcA (B3, B7 and C2), and $\delta^{13}C$ for *cis*-DCE, VC, 1,1-DCA and 1,1,1-TCA (B4, B5, B8 and C3).

resulting in high enrichment of $\delta^{13}C$ in *cis*-DCE. Combined biotic and abiotic transformation of TCE and *cis*-DCE was also found to proceed in an anaerobic microcosm experiment with sandstone (Darlington et al., 2008). Liang et al. (2007) reported strong carbon isotope fractionation during abiotic degradation of PCE (enrichment factor of −30.2‰) and TCE (enrichment factor of −33.4‰) by FeS. FeS can be formed during iron and sulfate reduction (Appelo and Postma, 2005). The reduced

conditions in the clay till (Fig. 2d) indicate that abiotic transformation of TCE by biotically mediated FeS can have occurred. In laboratory batch experiments Jeong et al. (2011) found that FeS did not react with *cis*-DCE, however, iron oxides such as green rust were highly reactive resulting in production of acetylene. Ferrey et al. (2004) found abiotic degradation of *cis*-DCE by magnetite in microcosm constructed with aquifer sediment. This suggests that abiotic degradation of *cis*-DCE by iron minerals can have occurred. However, further distinction between of the biotic and abiotic degradations of TCE and *cis*-DCE is limited by lack of an enrichment factor for abiotic *cis*-DCE degradation.

The low 1,1,1-TCA and high 1,1-DCA concentrations indicate significant degradation of 1,1,1-TCA to 1,1-DCA by reductive dechlorination (e.g. Sun et al., 2002). The presence of *Dhb* suggests that *Dhb* may be responsible for microbial reductive dechlorination of 1,1,1-TCA. No further degradation to CA apparently occurs, as CA was not detected. A very strong enrichment in the $\delta^{13}C$ value for 1,1,1-TCA (+25‰) was observed relative to an expected source isotope signature (range between −32‰ and −25‰ reported by Hunkeler et al., 2008). The availability of measured enrichment factors for 1,1,1-TCA in literature is limited. Lollar et al. (2010) determined an enrichment factor of −1.8‰ for microbial reductive dechlorination of 1,1,1-TCA to 1,1-DCA by a mixed culture containing *Dhb*. Elsner et al. (2007) found enrichment factors for abiotic degradation of 1,1,1-TCA by metals (Cr(II), Fe(0), Cu/Fe mix) of −15.8‰ to −13.7‰ indicating the involvement of a single C–Cl bond (likely by single electron transfer forming a dichloroethyl radical) in the initial rate limiting step. The low biotic enrichment factor observed by Lollar et al. (2010) indicates that the large expected kinetic isotope effect for C–Cl bond cleavage was almost completely masked by rate limiting steps preceding bond cleavage during biodegradation. Based on these findings, the very strong enrichment observed for 1,1,1-TCA in our study may suggest, that abiotic degradation has contributed to the degradation of 1,1,1-TCA.

Concurrent abiotic degradation of 1,1,1-TCA by α-dehaloelimination to 1,1-DCE (~27%) and by hydrolysis to acetate has been reported (see review by Scheutz et al., 2011). 1,1-DCE was not detected (<2 μmol/L) and its biotic degradation products VC and ethene were only detected in very low concentration relative to *cis*-DCE, which they were likely reductive dechlorination products from. Elsner and Hofstetter (2011) suggested another abiotic degradation pathway for 1,1,1-TCA via organochlorine radical (by single electron transfer) and/or carbanion with primarily non-chlorinated degradation products and potentially some 1,1-DCA depending on the presence of radical scavengers. This pathway is consistent with observed abiotic degradation of 1,1,1-TCA by FeS in studies by Choi et al. (2009) and Gander et al. (2002), where 1,1-DCA was found to account for 4–6% of the 1,1,1-TCA degraded.

The 1,1-DCA $\delta^{13}C$ values observed (~−20‰) were more enriched, than the expected 1,1,1-TCA source isotope signature. This might be explained by 1,1-DCA undergoing further degradation or by 1,1-DCA derived from previously enriched 1,1,1-TCA, i.e. by partial degradation by a different pathway predominantly leading to other products (than 1,1-DCA) such as abiotic reduction by FeS. As no CA was detected and redox conditions were consistent with FeS formation by iron and sulfate reduction, we speculate that initial abiotic degradation by FeS followed by microbial reductive dechlorination to 1,1-DCA may have taken place.

In summary, reductive dechlorination of TCE and 1,1,1-TCA to *cis*-DCE and 1,1-DCA respectively, has taken place in the core from borehole B. The presence of 1,1,1-TCA in part of the sub-section profile seems to inhibit further degradation of *cis*-DCE. A narrow zone of 10 cm with degradation to ethene was observed, but *Dhc* was not detected. The enriched $\delta^{13}C$ values of both chlorinated ethenes and ethanes indicate that both biotic and abiotic degradations have occurred in the sub-section profile.

4.2.3. Degradation of TCE to ethene in the clay till matrix

In the intact core from 11.00 to 11.50 m b.s. in borehole B a soft sandy clay till was found from 11.05 to 11.12 m b.s. (Fig. 5). The concentrations of the chlorinated ethenes were constant from the top of the soft clay till layer down to a depth of 11.28 m b.s. Below 11.28 m b.s., the concentrations of TCE and *cis*-DCE decrease while the concentrations of VC and ethene increase (Fig. 5B6). This indicates that TCE, *cis*-DCE and VC are degraded by reductive dechlorination. In the lower part the concentration profiles indicate that TCE is completely degraded to *cis*-DCE and *cis*-DCE is further degraded to VC (Fig. 5B6, from 11.32 to 11.42 m b.s.). TCE and *cis*-DCE are more enriched in $\delta^{13}C$ (−25‰ and −23‰ respectively) than in the upper part (−27‰ and −25‰ respectively) in correspondence with greater degradation (Fig. 5B7). VC is depleted in $\delta^{13}C$ suggesting only limited further degradation of VC consistent with the low ethene and ethane concentrations. The presence of *Dhb* in the clay till matrix (Fig. 5B7) suggests that these may have contributed to TCE reduction. However, the degradation to ethene was not supported by the presence of *Dhc* in the clay till matrix.

Dhc with the *vcrA* and *bvcA* genes were present in the high permeability features in the screen from 11 to 13 m b.s. in borehole B (2.1×10^7 cells/L, Table 1). In addition the groundwater samples showed activity of the specific genes (17 and 3 for *vcrA* and *bvcA*, respectively). The high number and activity of *vcrA* compared to *bvcA* indicates that *vcrA* is the dominating gene in the dechlorination to ethene (specific numbers given in Table 1). The activity of the *vcrA* gene is higher in borehole B compared to the screens in borehole C where the *vcrA* gene is also observed (Table 1). However, the number of *Dhc* present is similar (10^7 cells/L, specific numbers given in Table 1) illustrating that there is no correlation between the VC reductase gene numbers and the variation in *Dhc* which was also observed in a study by van der Zaan et al. (2010). Similar, to observations made by Carreón-Diazconti et al. (2009) the presence of bacteria and activity of the functional genes in the three boreholes at the site (see Table 1) are very heterogeneously distributed. The higher activity of *Dhc* with the *vcrA* gene in borehole B than in borehole C could likely be due to the more reduced conditions in borehole B which may be more favorable for *Dhc* with the *vcrA* gene.

In summary, an active sub-section of 10 cm with complete degradation of TCE to *cis*-DCE and partial degradation to VC and ethene was observed in the clay till matrix in borehole B. The presence of *Dhb* in the clay till matrix suggests that these can have carried out degradation of TCE to *cis*-DCE. Degradation of *cis*-DCE to VC was documented by

enriched $\delta^{13}C$ for *cis*-DCE, but *Dhc* were not detected. Groundwater from the screen in same depth showed that *Dhc* with the *vcrA* gene were present and active in the high permeability features.

4.2.4. Degradation of PCE to ethene in the clay till matrix

In the intact core from 5.60 to 6.00 m b.s. from borehole C a soft clay till layer extended from 5.6 to 5.63 m b.s. (Fig. 5). The rest of the core consisted of massive and firm clay till. PCE, TCE and *cis*-DCE were found in highest concentrations close to the soft clay till (Fig. 5C1). The concentrations are decreasing downwards in the more firm clay till matrix. In the depth interval from 5.68–5.74 m b.s., the concentrations of PCE decrease with depth while *cis*-DCE increases. This indicates reductive dechlorination of PCE through TCE to *cis*-DCE. Degradation of PCE and TCE can potentially be carried out by *Dhb* (Middeldorp et al., 1999) and these are present in the clay till matrix (Fig. 5C2). $\delta^{13}C$ for PCE, TCE and *cis*-DCE are all enriched compared to $\delta^{13}C_0$ (expected to be approximately −30‰ for TCE at the site) (Fig. 5C3) indicating degradation of all three compounds. The strong enrichment of $\delta^{13}C$ for and low concentration of TCE compared to PCE indicate that TCE is degraded concurrently with PCE. It also indicates that TCE is an intermediate degradation product and not the mother product in well C in contrast to wells A and B (see location on Fig. 1a). The $\delta^{13}C$ value for *cis*-DCE increases from −18‰ in the soft clay till (5.65 m b.s.) to −14‰ in the firm clay till (5.98 m b.s.) (Fig. 5C3) indicating that degradation of *cis*-DCE is also taking place in the firm clay till matrix. The presence of both VC and ethene in the sub-section profile indicates that complete dechlorination occurs. Degradation to ethene is strongly supported by the presence of the VC reductase gene *vcrA* until 5.73 m b.s. (Fig. 5C2). The number of *vcrA* genes decreases from the top of the sub-section profile and into the clay till matrix. *Dhc* were only found in the upper part (extending down to 5.65 m b.s.) of the soft clay till whereas they were not detected below this depth (Fig. 5C2). *Dhc* were also present in the groundwater from the screen in 5.50–5.80 m b.s. (Table 1). This may suggest that degradation developed in the high permeability features where the right conditions first evolved and then progressed into the soft clay till matrix.

To summarize, an active sub-section with reductive dechlorination of PCE to ethene up to approximately 13 cm was observed in soft clay till as well as in the high permeability features represented by groundwater samples. The reductive dechlorination to ethene was documented by the presence of *Dhb*, *Dhc* and the VC reductase gene *vcrA* in the soft clay till and $\delta^{13}C$ enrichment of PCE, TCE and *cis*-DCE.

5. Conclusions

A large spatial variability in the distribution and composition of the chlorinated ethenes and ethanes in the source zone at the site was observed in the groundwater and in the clay till matrix. This reveals that the release of contaminants and the subsequent transport in the clay till are complex and affected by preferential pathways (sand stringers, lenses and fractures) identified in the clay till. Transport in the clay till matrix was controlled by diffusion. Desorption or dissolution of residual phase TCE was taking place at borehole A. At boreholes B and C the dominance of *cis*-DCE and 1,1-DCA in both high permeability features and the clay till matrix documents that PCE, TCE and 1,1,1-TCA were undergoing degradation at the site. Sections with partial degradation of *cis*-DCE were also identified.

High resolution core profiles from the clay till matrix showed reductive degradation of PCE and TCE. Degradation was primarily to *cis*-DCE but there were sporadically distributed sub-sections of the cores where active degradation to ethene was identified. Biotic as well as abiotic degradations were identified by CSIA analysis in one sub-section. Abiotic degradation may potentially proceed by reaction with reduced iron minerals. The dominating microbial specie in the clay till matrix was *Dhb*, which supports that degradation in most cases stagnates at *cis*-DCE. *Dhc* with the VC reductase gene *vcrA* were detected in one (borehole C) out of four active sub-sections with degradation to ethene. In sections where *Dhc* were not detected, concentration profiles, presence of VC and ethene and enriched $\delta^{13}C$ for *cis*-DCE and VC indicate that *Dhc* may have been present, but if they were present their density was below the detection limit. *Dhc* with the *vcrA* and *bvcA* gene were present and active in the high permeability features from borehole B and the deeper screens of borehole C.

The high resolution sampling reveals a complex system where diffusion, biotic and abiotic degradation processes occur in parallel in both the high permeability features and the clay till matrix after several decades of contamination. Diffusion and biotic degradation of chlorinated compounds were observed from concentration profiles of chlorinated ethenes and the microbes present in the clay till matrix. CSIA measurements gave a unique possibility to identify abiotic and biotic degradation processes of chlorinated ethenes and ethanes in situ. To quantify and in some cases distinguish between diffusion, biotic and abiotic degradation processes application of reactive transport modeling accounting for isotope enrichment could be beneficial. Currently, we are working along these lines; however, the lack of knowledge regarding initial conditions in the clay till system and enrichment factors for abiotic degradation processes poses a challenge.

The findings in this study have significant implications for application of enhanced reductive dechlorination at clay till sites. The results show on one hand promises for enhancement of microbial activity in the clay till matrix and on the other hand reveal a very complex and heterogeneous development of bioactive zones.

Acknowledgments

The presented research is part of the research project *Innovative Remediation and Assessment Technologies for Contaminated Soil and Groundwater* (REMTEC). The project is carried out in collaboration with the Capital Region of Denmark and the consulting company Orbicon. We thank Jens Schaarup, Mona Refstrup, and Bent Skov at DTU Environment; Kresten Andersen at Orbicon; Carsten Bagge Jensen and Henriette Kerrn-Jespersen at the Capital Region of Denmark for their contributions.

Appendix A. Supplementary data

Supplementary data to this article can be found online at http://dx.doi.org/10.1016/j.jconhyd.2012.11.010.

References

Amos, B.K., Christ, J.A., Abriola, L.M., Pennell, K.D., Loffler, F.E., 2007. Experimental evaluation and mathematical modeling of microbially enhanced tetrachloroethene (PCE) dissolution. Environmental Science & Technology 41 (3), 963–970.

Appelo, C.A.J., Postma, D., 2005. Geochemistry, groundwater and pollution, 2nd edition. A.A. Balkema Publishers0415364280.

Aulenta, F., Pera, A., Rossetti, S., Papini, M.P., Majone, M., 2007. Relevance of side reactions in anaerobic reductive dechlorination microcosms amended with different electron donors. Water Research 41 (1), 27–38.

Capital Region of Denmark, 2007. Vasbyvej 16A—supplementing investigations. (in Danish) Orbicon for Capital Region of Denmark.

Carreón-Diazconti, C.ü., Santamariá, J., Berkompas, J., Field, J.A., Brusseau, M.L., 2009. Assessment of in situ reductive dechlorination using compound-specific stable isotopes, functional gene PCR, and geochemical data. Environmental Science & Technology 43 (12), 4301–4307.

Chambon, J.C., Broholm, M.M., Binning, P.J., Bjerg, P.L., 2010. Modeling multicomponent transport and enhanced anaerobic dechlorination processes in a single fracture–clay matrix system. Journal of Contaminant Hydrology 112 (1–4), 77–90.

Chamier, B., Lorenz, M.G., Wackernagel, W., 1993. Natural transformation of acinetobacter calcoaceticus by plasmid DNA adsorbed on sand and groundwater aquifer material. Applied and Environmental Microbiology 59 (5), 1662–1667.

Chan, W.W.M., Grostern, A., Löffer, F.E., Edwards, E.A., 2011. Quantifying the effects of 1,1,1-trichloroethane and 1,1-dichloroethane on chlorinated ethene reductive dehalogenases. Environmental Science & Technology 45 (22), 9693–9702.

Chartrand, M.M.G., Morrill, P.L., Lacrampe-Couloume, G., Lollar, B.S., 2005. Stable isotope evidence for biodegradation of chlorinated ethenes at a fractured bedrock site. Environmental Science & Technology 39 (13), 4848–4856.

Choi, J., Choi, K., Lee, W., 2009. Effects of transition metal and sulfide on the reductive dechlorination of carbon tetrachloride and 1,1,1-trichloroethane by FeS. Journal of Hazardous Materials 162 (2–3), 1151–1158.

Christiansen, C.M., Riis, C., Christensen, S.B., Broholm, M.M., Christensen, A.G., Klint, K.E.S., Wood, J.S.A., Bauer-Gottwein, P., Bjerg, P.L., 2008. Characterization and quantification of pneumatic fracturing effects at a clay till site. Environmental Science & Technology 42 (2), 570–576.

Christiansen, C.M., Damgaard, I., Broholm, M., Kessler, T., Klint, K.E., Nilsson, B., Bjerg, P.L., 2010. Comparison of delivery methods for enhanced in situ remediation in clay till. Ground Water Monitoring & Remediation 30 (4), 107–122.

Courbet, C., Rivire, A.s., Jeannottat, S., Rinaldi, S., Hunkeler, D., Bendjoudi, H., de Marsily, G., 2011. Complementing approaches to demonstrate chlorinated solvent biodegradation in a complex pollution plume: mass balance, PCR and compound-specific stable isotope analysis. Journal of Contaminant Hydrology 126 (3–4), 315–329.

Damgaard, I., Bjerg, P.L., Jacobsen, C.S., Tsitonaki, A., Kernn-Jespersen, H., Broholm, M.M., 2012. Performance of full scale bioremediation in clay till using enhanced reductive dechlorination. Ground Water Monitoring & Remediation. http://dx.doi.org/10.1111/j1745-6592.2012.01405.x.

Darlington, R., Lehmicke, L., Andrachek, R.G., Freedman, D.L., 2008. Biotic and abiotic anaerobic transformations of trichloroethene and *cis*-1,2-dichloroethene in fractured sandstone. Environmental Science & Technology 42 (12), 4323–4330.

Dearden, R.A., Noy, D.J., Lelliott, M.R., Wilson, R., Wealthall, G.P., 2012. Release of contaminants from a heterogeneously fractured low permeability unit underlying a DNAPL source zone. Journal of Contaminant Hydrology (0). http://dx.doi.org/10.1016/j.jconhyd.2011.05.006.

Duhamel, M., Wehr, S.D., Yu, L., Rizvi, H., Seepersad, D., Dworatzek, S., Cox, E.E., Edwards, E.A., 2002. Comparison of anaerobic dechlorinating enrichment cultures maintained on tetrachloroethene, trichloroethene, *cis*-dichloroethene and vinyl chloride. Water Research 36 (17), 4193–4202.

Elsner, M., Hofstetter, T.B., 2011. Current perspectives on the mechanism of chlorohydrocarbon degradation in subsurface environments: insights from kinetics, product formation, probe molecules and isotope fractionation. In: Tratnyak, P., et al. (Ed.), Aquatic Redox Chemistry. American Chemical Society, Washington D.C., pp. 407–439 (Chapter A).

Elsner, M., Cwirtny, D.M., Roberts, A.L., Lollar, B.S., 2007. 1,1,2,2-Tetrachloroethane reactions with OH-, Cr(II), granular iron, and copper–iron bimetal: insights from product formation and associated carbon isotope fractionation. Environmental Science & Technology 41 (11), 4111–4117.

ESTCP, 2004. Principles and practices of enhanced anaerobic bioremediation of chlorinated solvents. Air Force Center for Environmental Excellence, Naval Facilities Engineering Service Center and Environmental Security Technology Certification Program.

Falta, R.W., 2005. Dissolved chemical discharge from fractured clay aquitards contaminated with DNPALs. In: Faybishenko, B. (Ed.), Dynamic of Fluids and Transport in Fractured Rock. Geophysical Monograph, 162. American Geophysical Union, Washington, DC, pp. 165–174.

Ferrey, M.L., Wilkin, R.T., Ford, R.G., Wilson, J.T., 2004. Nonbiological removal of *cis*-dichloroethylene and 1,1-dichloroethylene in aquifer sediment containing magnetite. Environmental Science & Technology 38 (6), 1746–1752.

Gander, J.W., Parkin, G.F., Scherer, M.M., 2002. Kinetics of 1,1,1-trichloroethane transformation by iron sulfide and a methanogenic consortium. Environmental Science & Technology 36 (21), 4540–4546.

Grostern, A., Edwards, E.A., 2006. A 1,1,1-trichloroethane-degrading anaerobic mixed microbial culture enhances biotransformation of mixtures of chlorinated ethenes and ethanes. Applied and Environmental Microbiology 72 (12), 7849–7856.

He, Y.T., Wilson, J.T., Wilkin, R.T., 2008. Transformation of reactive iron minerals in a permeable reactive barrier (biowall) used to treat TCE in groundwater. Environmental Science & Technology 42 (17), 6690–6696.

He, Y.T., Wilson, J.T., Wilkin, R.T., 2010. Impact of iron sulfide transformation on trichloroethylene degradation. Geochimica et Cosmochimica Acta 74, 2025–2039.

Heimann, A.C., Friis, A.K., Jakobsen, R., 2005. Effects of sulfate on anaerobic chloroethene degradation by an enriched culture under transient and steady-state hydrogen supply. Water Research 39 (15), 3579–3586.

Heron, G., Crouzet, C., Bourg, A.C.M., Christensen, T.H., 1994. Speciation of Fe(Ii) and Fe(Iii) in contaminated aquifer sediments using chemical-extraction techniques. Environmental Science & Technology 28 (9), 1698–1705.

Hoelen, T.P., Reinhard, M., 2004. Complete biological dehalogenation of chlorinated ethylenes in sulfate containing groundwater. Biodegradation 15 (6), 395–403.

Hunkeler, D., Aravena, R., Berry-Spark, K., Cox, E., 2005. Assessment of degradation pathways in an aquifer with mixed chlorinated hydrocarbon contamination using stable isotope analysis. Environmental Science & Technology 39 (16), 5975–5981.

Hunkeler, D., Meckenstock, R., Lollar, B.S., Wilson, J.T., 2008. A Guide for Assessing Biodegradation and Source Identification of Organic Ground Water Contamination Using Compound Specific Isotope Analysis (CSIA). EPA, United States Environmental Protection Agency.

Hunkeler, D., Abe, Y., Broholm, M.M., Jeannottat, S., Westergaard, C., Jacobsen, C.S., Aravena, R., Bjerg, P.L., 2011. Assessing chlorinated ethene degradation in a large scale contaminant plume by dual carbon–chlorine isotope analysis and quantitative PCR. Journal of Contaminant Hydrology 119 (1–4), 69–79.

Jeong, H.Y., Anantharaman, K., Han, Y.S., Hayes, K.F., 2011. Abiotic reductive dechlorination of *cis*-dichloroethylene by Fe species formed during iron- or sulfate-reduction. Environmental Science & Technology 45 (12), 5186–5194.

Kniemeyer, O., Musat, F., Sievert, S.M., Knittel, K., Wilkes, H., Blumenberg, M., Michaelis, W., Classen, A., Bolm, C., Joye, S.B., Widdel, F., 2007. Anaerobic oxidation of short-chain hydrocarbons by marine sulphate-reducing bacteria. Nature 449 (7164), 898–901.

Lee, W., Batchelor, B., 2002a. Abiotic reductive dechlorination of chlorinated ethylenes by iron-bearing soil minerals. 2. Green rust. Environmental Science & Technology 36 (24), 5348–5354.

Lee, W., Batchelor, B., 2002b. Abiotic reductive dechlorination of chlorinated ethylenes by iron-bearing soil minerals. 1. Pyrite and magnetite. Environmental Science & Technology 36 (23), 5147–5154.

Lemming, G., Hauschild, M.Z., Chambon, J., Binning, P.J., Bulle, C., Margni, M., Bjerg, P.L., 2010. Environmental impacts of remediation of a trichloroethene-contaminated site: life cycle assessment of remediation alternatives. Environmental Science & Technology 44 (23), 9163–9169.

Liang, X., Dong, Y., Kuder, T., Krumholz, L.R., Philp, R.P., Butler, E.C., 2007. Distinguishing abiotic and biotic transformation of tetrachloroethylene and trichloroethylene by stable carbon isotope fractionation. Environmental Science & Technology 41, 7094–7100.

Lollar, B.S., Slater, G.F., Sleep, B., Witt, M., Klecka, G.M., Harkness, M., Spivack, J., 2001. Stable carbon isotope evidence for intrinsic bioremediation of tetrachloroethene and trichloroethene at area 6, Dover Air Force Base. Environmental Science & Technology 35 (2), 261–269.

Lollar, B.S., Hirschorn, S., Mundle, S.O.C., Grostern, A., Edwards, E.A., Lacrampe-Couloume, G., 2010. Insights into enzyme kinetics of chloroethane biodegradation using compound specific stable isotopes. Environmental Science & Technology 44 (19), 7498–7503.

Lovley, D.R., Phillips, E.J.P., 1987. Rapid assay for microbially reducible ferric iron in aquatic sediments. Applied and Environmental Microbiology 1536–1540.

Lu, C., Bjerg, P.L., Zhang, F., Broholm, M.M., 2011. Sorption of chlorinated solvents and degradation products on natural clayey tills. Chemosphere 83 (11), 1467–1474.

Major, D.W., McMaster, M.L., Cox, E.E., Edwards, E.A., Dworatzek, S.M., Hendrickson, E.R., Starr, M.G., Payne, J.A., Buonamici, L.W., 2002. Field demonstration of successful bioaugmentation to achieve dechlorination of tetrachloroethene to ethene. Environmental Science & Technology 36 (23), 5106–5116.

Manoli, G., Chambon, J., Broholm, M.M., Scheutz, C., Binning, P.J., Bjerg, P.L., 2011. A remediation performance model for enhanced metabolic reductive dechlorination of chloroethenes in fractured clay till. Journal of Contaminant Hydrology 131 (1–4), 64–78.

MaymoGatell, X., Tandoi, V., Gossett, J.M., Zinder, S.H., 1995. Characterization of an H-2-utilizing enrichment culture that reductively dechlorinates tetrachloroethene to vinyl-chloride and ethene in the absence of methanogenesis and acetogenesis. Applied and Environmental Microbiology 61 (11), 3928–3933.

MaymoGatell, X., Chien, Y.T., Gossett, J.M., Zinder, S.H., 1997. Isolation of a bacterium that reductively dechlorinates tetrachloroethene to ethene. Science 276 (5318), 1568–1571.

Middeldorp, P.J.M., Luijten, M.L.G.C., van de Pas, B.A., Eekert, M.H.A., Kengen, S.W.M., Schraa, G., Stams, A.J.M., 1999. Anaerobic microbial reductive dehalogenation of chlorinated ethenes. Bioremediation Journal 3 (3), 151–169.

Muller, J.A., Rosner, B.M., von Abendroth, G., Meshulam-Simon, G., McCarty, P.L., Spormann, A.M., 2004. Molecular identification of the catabolic vinyl chloride reductase from *Dehalococcoides* sp. strain VS and its environmental distribution. Applied and Environmental Microbiology 70 (8), 4880–4888.

Parker, B.L., Cherry, J.A., Chapman, S.W., 2004. Field study of TCE diffusion profiles below DNAPL to assess aquitard integrity. Journal of Contaminant Hydrology 74 (1–4), 197–230.

Reynolds, D.A., Kueper, B.H., 2002. Numerical examination of the factors controlling DNAPL migration through a single fracture. Ground Water 40 (4), 368–377.

Sabalowsky, A.R., Semprini, L., 2010. Trichloroethene and *cis*-1,2-dichloroethene concentration-dependent toxicity model simulates anaerobic dechlorination at high concentrations: I. Batch-fed reactors. Biotechnology and Bioengineering 107 (3), 529–539.

Scheutz, C., Durant, N.D., Dennis, P., Hansen, M.H., Jorgensen, T., Jakobsen, R., Cox, E.E., Bjerg, P.L., 2008. Concurrent ethene generation and growth of *Dehalococcoides* containing vinyl chloride reductive dehalogenase genes during an enhanced reductive dechlorination field demonstration. Environmental Science & Technology 42 (24), 9302–9309.

Scheutz, C., Broholm, M.M., Durant, N.D., Weeth, E.B., Jorgensen, T.H., Dennis, P., Jacobsen, C.S., Cox, E.E., Chambon, J.C., Bjerg, P.L., 2010. Field evaluation of biological enhanced reductive dechlorination of chloroethenes in clayey till. Environmental Science & Technology 44 (13), 5134–5141.

Scheutz, C., Durant, N.D., Hansen, M.H., Bjerg, P.L., 2011. Natural and enhanced anaerobic degradation of 1,1,1-trichloroethane and its degradation products in the subsurface—a critical review. Water Research 45 (9), 2701–2723.

Seshadri, R., Adrian, L., Fouts, D.E., Eisen, J.A., Phillippy, A.M., Methe, B.A., Ward, N.L., Nelson, W.C., Deboy, R.T., Khouri, H.M., Kolonay, J.F., Dodson, R.J., Daugherty, S.C., Brinkac, L.M., Sullivan, S.A., Madupu, R., Nelson, K.T., Kang, K.H., Impraim, M., Tran, K., Robinson, J.M., Forberger, H.A., Fraser, C.M., Zinder, S.H., Heidelberg, J.F., 2005. Genome sequence of the PCE-dechlorinating bacterium *Dehalococcoides ethenogenes*. Science 307 (5706), 105–108.

Sun, B.L., Griffin, B.M., yala-del-Rio, H.L., Hashsham, S.A., Tiedje, J.M., 2002. Microbial dehalorespiration with 1,1,1-trichloroethane. Science 298 (5595), 1023–1025.

Sung, Y., Ritalahti, K.M., Apkarian, R.P., Loffler, F.E., 2006. Quantitative PCR confirms purity of strain GT, a novel trichloroethene-to-ethene-respiring *Dehalococcoides* isolate. Applied and Environmental Microbiology 72 (3), 1980–1987.

Takeuchi, M., Kawabe, Y., Watanabe, E., Oiwa, T., Takahashi, M., Nanba, K., Kamagata, Y., Hanada, S., Ohko, Y., Komai, T., 2011. Comparative study of microbial dechlorination of chlorinated ethenes in an aquifer and a clayey aquitard. Journal of Contaminant Hydrology 124 (1–4), 14–24.

van der Zaan, B., Hannes, F., Hoekstra, N., Rijnaarts, H., de Vos, W.M., Smidt, H., Gerritse, J., 2010. Correlation of *Dehalococcoides* 16S rRNA and chloroethene-reductive dehalogenase genes with geochemical conditions in chloroethene-contaminated groundwater. Applied and Environmental Microbiology 76 (3), 843–850.

Wei, N., Finneran, K.T., 2011. Influence of ferric iron on complete dechlorination of trichloroethylene (TCE) to ethene: Fe(III) reduction does not always inhibit complete dechlorination. Environmental Science & Technology 45 (17), 7422–7430.